Journal of Hydrology 597 (2021) 126199

Contents lists available at ScienceDirect

Journal of Hydrology

journal homepage: www.elsevier.com/locate/jhydrol

Research papers

Seasonal transpiration dynamics of evergreen *Ligustrum lucidum* linked with water source and water-use strategy in a limestone karst area, southwest China

Ze Wu, Hamid M. Behzad [1], Qiufang He, Chao Wu, Ying Bai, Yongjun Jiang [*]

Chongqing Key Laboratory of Karst Environment & School of Geographical Sciences of Southwest University, Chongqing 400715, China

ARTICLE INFO

Keywords:
Seasonal transpiration
Sap flow
Stable isotopes
WUE_i
Deep water
Limestone karst area

ABSTRACT

Transpiration dynamics of karst ecosystems are not conditioned only by the shallow-soil water status, mainly because of the presence of deep-water source pools formed within the underlying bedrock if trees can develop their deep roots to the pools. However, the strength of these relationships and how as well as why they can vary from an area to another and from season to season are poorly understood, due primarily to high heterogeneity of karst ecosystems. Therefore, the present study was conducted during 2018–2019 rainy and dry seasons in a subtropical (limestone) karst area on southwest China to explore the functional responses to reduced water availability of evergreen *Ligustrum lucidum* (Chinese glossy privet) growing on the shallow soils. Seasonal variations in the transpiration, water-use patterns, and water sources were investigated for *Ligustrum lucidum* through high-resolution monitoring of the micrometeorology, sap flow, and soil moisture data, in combination with the carbon stable isotope composition of the tree leaves, as well as oxygen and hydrogen stable isotope composition of the tree stem, soil, and deep water. Our findings showed that high transpiration rates of *Ligustrum lucidum* were mainly associated with the soil moisture during rainy seasons (87% in total) but the low rates were associated primarily with the deep-water sources during dry seasons (13% in total). During the rainy season, when plenty of water was available to the plant, *Ligustrum lucidum* tended to obtain water inexpensively through the soil layers (on average, 59%) and consumed it profligately through reduction of its water use efficiency (WUE_i) (mean $WUE_{i\ rainy\text{-}season} = 82.6$ μmol/mol). In contrast, during the dry season, when limited water was available to the plant resulting from the significant reduction in rainfall, *Ligustrum lucidum* had to obtain the water expensively (albeit at a small amount) through deep-water source pools (on average, 62%), and consumed it conservatively through increasing its WUE_i (mean $WUE_{i\ rainy\text{-}season} = 108.6$ μmol/mol). Our findings can provide the insights into temporal transpiration dynamics as well as the strategies and mechanisms adopted by the plants to counteract the seasonal drought stress associated with the shallow soils in karst ecosystems.

1. Introduction

Karst landforms are a major natural landscape, covering an area of over 22 million km^2 worldwide (Ford and Williams, 2007). A unique karst (limestone) landscape can be found in Southwest China, with an area of approximately 500,000 km^2 (Yuan, 1994). This area is highly heterogeneous, with non-continuous shallow soil (average depth of less than 50 cm) from the underlying limestone (Rong et al., 2011; Liu et al., 2019). Additionally, shallow soils are often underlain by fractured bedrock, resulting in a high percolation capacity and low water-holding capacity in the soil layers (Rong et al., 2011; Jiang et al., 2014; Yan et al., 2019). Although this humid subtropical monsoon region receives an average annual rainfall of over 1000 mm, it experiences an annual four- or five-month drought often between November and March (Nie et al., 2012). These conditions may individually lead to drought (water) stress that can limit the survival, growth and distribution of karst vegetation species, particularly during prolonged drought periods (White et al., 1985; Jackson, et al., 1999; McCole and Stern, 2007; Querejeta et al., 2007; Hasselquist et al., 2010; Rong et al., 2011; Heilman et al., 2014; Nie et al., 2011, 2014; Cao et al., 2020).

Transpiration is a critical physiological mechanism involved in water conservation strategies, which allows for plant growth and survival

* Corresponding author.
E-mail address: jiangjyj@swu.edu.cn (Y. Jiang).
[1] Joint first author.

https://doi.org/10.1016/j.jhydrol.2021.126199

Available online 16 March 2021

(Nobel, 2005; Muñoz-Villers et al., 2018). Thus, investigating the transpiration process under the conditions of water deficiency will provide necessary information on the responses of the plant to variations in the atmospheric and soil moisture conditions (Greco and Baldocchi, 1996; Oren and Pataki, 2001). The way through which the plants increase, maintain, or decrease transpiration all-year-round is different in karst areas than the non-karst areas, and usually depends on two key factors: rooting depth and water availability in the lower root zone of the trees. In the non-karst areas, where the soil layers can be thick, roots can easily grow in the soil because of the sufficient water strongly influencing the plant transpiration (Alarcón et al., 2000; Oren and Pataki, 2001). However, in karst areas, despite the thin soil layer with limited water storage, many endemic trees have been found to be relatively insensitive to the upper-soil drought conditions due to the ability to have access to the water from deeper sources (Jackson et al., 2000; Querejeta et al., 2007; Schwinning, 2010; Huang et al., 2011; Estrada-Medina et al., 2013; Carrière et al., 2020). For example, Pockman et al. (2008) found that during the prolonged drought, plants can take up to 60% of total daily transpiration through their deep roots from the bedrock fissure under the karst of the Edwards Plateau, Texas, US. Additionally, Huang et al. (2009) demonstrated that in a karst landscape vegetated by Cyclobalanopsis glauca transpiration was high, which the highest contribution of water source was from epikarst during the dry season. In addition to the mechanism of deep root development mentioned above, there are several other mechanisms and strategies that can influence the plant transpiration including the increase in intrinsic water use efficiency (WUE_i) (Moreno-Gutiérrez et al., 2012; Olano et al., 2014; Cao et al., 2020), formation of the leaves with thicker cuticles or waxy layers and well-developed epidermal hairs (Barbeta & Peñuelas, 2016), decreasing the stomatal conductance and photosynthetic rates (Moreno-Gutiérrez et al., 2012; Martínez-Vilalta et al., 2014; Rumman et al., 2017), or even reducing the growth rate (Olano et al., 2014). However, the nature of transpiration dynamics, transpired water sources, and water-use strategies for trees in the karst ecosystems may vary from an area to another as well as from season to season primarily due to high heterogeneity of karst ecosystems.

To date, several techniques have been employed to explore the mechanisms and strategies adopted by plants. A large number of studies have used plant WUE—the ratio of carbon assimilated to water transpired by plant—inferred from $\delta^{13}C$ signatures (i.e., the ratio of ^{13}C to ^{12}C) of plant leaves and other materials to analyze plant performance under different water stress conditions (Querejeta et al., 2006; Cernusak et al., 2013; Nie et al., 2014; Esmaeilpour et al., 2016; Rumman et al., 2017; Cao et al., 2020; Ding et al., 2020). At the leaf scale, WUE_i—the ratio of net assimilation to stomatal conductance—was included to identify photosynthetic properties independent of (or at a common) evaporative demand (Osmond et al., 1980). A simplified linear model (Farquhar et al., 1982) was often used to estimate the leaf-scale WUE_i, to the value of which it is negatively correlated with photosynthetic ^{13}C discrimination (Δ) and positively with C_i/C_a (i.e., the ratio of intercellular to ambient CO_2 partial pressures). Besides, this linear model could be explicitly linked the performance of plant WUE with water availability in C_3 plants (Craven et al. 2013), whereby their high WUE are reflected in less negative $\delta^{13}C$ and low C_i/C_a and vice versa (Farquhar & Richards, 1984; Dawson et al., 2002; Seibt et al., 2008). Therefore, WUE_i derived from stable carbon isotope ratios ($\delta^{13}C$) of plant tissues is frequently used as indicator of long-term trends in the internal regulation of carbon uptake and water loss of plants (Chaves et al., 2004; Seibt et al., 2008; Leonardi et al., 2012; Hu et al., 2019). On the other hand, analyses of stable oxygen ($\delta^{18}O$) and hydrogen ($\delta^{2}H$) isotope ratios determine potential water sources used by plants (White et al., 1985; Ehleringer and Dawson, 1992; Ogle et al., 2014; Barbeta et al., 2015; Evaristo et al., 2016, 2017; Liu et al., 2019). It has been assumed that no isotopic fractionation occurs when water enters the roots and therefore, helps estimating the mixing ratio of xylem water from different water sources (White et al., 1985; Ehleringer & Dawson, 1992; Dawson et al., 2002; McDonnell, 2014; Evaristo et al., 2017; Carrière et al., 2020). Various mixing models based on dual isotope ratio approach have been developed for the apportioning of water sources used by plant, including linear mixing models (e.g., IsoSource, Phillips & Gregg, 2003) and Bayesian mixing model (e.g., MixSIAR, Stock & Semmens, 2013; MixSIR, Moore & Semmens, 2008; and SIAR, Parnell et al., 2010; and IsotopeR, Hopkins & Ferguson, 2012). These multisource mixing models have been efficacious for the apportioning of plant water sources in complex natural ecosystems such as karst ecosystems where there are often more than two water sources for plant use (McCole & Stern, 2007; Rong et al., 2011; Nie et al., 2012; Liu et al., 2019). However, a number of factors are at play to decide which stable isotope mixing model (SIMM) to apply including mixtures and sources (assemblages of single or multiple populations), sample sizes, researcher's intended level of inference (e.g., individual- or population-level), and users' familiarity with a particular framework to develop more efficient approaches for statistical analysis. For example, IsotopeR's user interface (in R) provides researchers with a user-friendly tool for SIMM analysis, and can incorporate all substantial SIMM features (i.e., components of the model expressed in mathematical terms) using a fully Bayesian approach to more accurately infer relative contributions for sources (Hopkins & Ferguson, 2012). This model also allows a user to make statistical inference on each individual in the population, even when there may be only one observation for each individual. Additionally, the model structure allows for incorporating replicated observations of the same individual in the analysis process, resulting in less influence from the population-level and more accurate individual-level estimates. Therefore, the model has a hierarchical structure as its point estimates is contingent on the group or population's distribution (Hopkins & Ferguson, 2012). Notably, like other SIMMs, this model adopts the same basic methodology for identifying plant water source apportionment. For example, a duel isotope (e.g., $\delta^{18}O$ and $\delta^{2}H$), multiple-endmember linear mixing model can be formulated for estimating the relative contribution (f) of multiple water sources (1, 2, 3…n) to a mixture of stem water (m) based on the following mass balance equations (Schwarcz, 1991):

$$\delta^{18}_m O = f_1\delta^{18}_1 O + f_2\delta^{18}_2 O + f_3\delta^{18}_3 O + \ldots f_n\delta^{18}_n O \quad (1)$$

$$\delta^{2}_m \mathrm{H} = f_1\delta^{2}_1 \mathrm{H} + f_2\delta^{2}_2 \mathrm{H} + f_3\delta^{2}_3 H + \ldots f_n\delta^{2}_n \mathrm{H} \quad (2)$$

$$f_1 + f_2 + f_3 + \ldots + \ + f_n = 1 \quad (3)$$

where, f_i is the relative source contributions to a mixture (m), and $\delta^{18}_{m,i}O$ and $\delta^{2}_{m,i}H$ are the isotope signatures for mixtures and sources, respectively.

Quantifying stand-scale transpiration via monitoring the sap flow of a single tree in a field has been another technique of interest in plant water-use research for the past two decades (Wilson et al., 2001; Kumagai et al., 2007; Du et al., 2011; Chang et al., 2014; Miyazawa et al., 2014; Liu et al., 2018; Han et al., 2019). The sap flow measurements, which is not restricted by the spatio-temporal variability (Link et al., 2014), allows us to determine the total quantity of water transpired by tree species on a daily basis, as well as to characterize the ecological and physiological mechanisms that tree species use to cope with limited availability of soil water (Pataki et al., 2000; Du et al., 2011; Huang et al., 2011; Berry et al., 2017). Although the combined use of these techniques is strongly emphasized in exploring the mechanisms and strategies that tree species use to adapt and survive in environments with various water stresses, it has not always been possible due to rising costs of sampling and analysis.

The present study was conducted during 2018–2019 rainy and dry seasons in a subtropical (limestone) karst area on southwest China to explore transpiration responses and water-use strategies of a dominant woody plant species (evergreen *Ligustrum lucidum*)—growing in a habitat with the typical shallow soils—using sap flow transpiration data,

leaf $\delta^{13}C$, and xylem (i.e., plant stem) and source water $\delta^{2}H$ and $\delta^{18}O$. This study aimed to achieve the following: (1) quantifying the amount of water transpired by the plant during different seasons; (2) revealing the nature of potential water sources providing the water needed for plant transpiration during different seasons; (3) determining the contributions and seasonal patterns of different potential water sources used by the plant; and (4) determining the plant WUE_i and its seasonal patterns.

2. Materials and methods

2.1. Study site

The Longfeng karst trough valley (106°25′22″-106°28′06″ E, 29°45′35″-29°49′02″ N), belonging to the northern part of the Zhongliang Mountain located in the Guanyinxia anticline, Chongqing, Southwest China (Fig. 1a, 1b), was chosen as the site of this study. The altitude of the Longfeng karst trough valley ranges from 480 to 640 m, and it covers an area of 11.7 km^2 with three ridges and two valleys. The limestone and dolomite components of the Lower Triassic Feixianguan Formation (T_1f) and Middle Triassic Leikoupo Formation (T_2l) formed the karst trough valleys, and the erosion-resistant sandstone and shale components of T_1f and the Upper Triassic Xujiahe Formation (T_3xj) formed the ridges (Fig. 1b). A dense network of open fractures has been developed in the limestone bedrock of the karst trough valleys, providing the basic conditions for the development of karst forms, such as fissures, sinkholes, karst pits, and underground rivers. Rainwater and surface water are quickly discharged into karst aquifers through fissures, sinkholes, or karst pits, and eventually into underground rivers, which can limit the storage of available water for plants in shallow zones.

The Longfeng Valley is affected by a humid subtropical monsoon climate, with an annual mean air temperature of 18.2 °C and precipitation of 1104 mm. Approximately, 75–85% of the annual precipitation occurs during the rainy season from April to October. The soil in the study site is thin with a depth of 10–50 cm. The soil types are mainly clay and silt which have covered most highly fractured bedrock outcrops. The forest land is the main land use, and its vegetation is mostly evergreen woody plant species, *Ligustrum lucidum (also known as Chinese glossy privet)*, *Cinnamomum camphora*, *Robinia pseudoacacia*, and *Celtis sinensis*. Most trees are over 20 years of age. Detailed information regarding the study area was presented in Liu et al. (2019).

Fig. 1(a) Geographic location of the study area; (b) Hydrological geology, and sampling points in the study area; (c) *Ligustrum lucidum*; (d) Sap flow measurement.

2.2. Measurement of microclimatic parameters

Various climatic parameters including precipitation (*P*), air temperature (*T*), relative humidity (*RH*), and solar radiation (R_s) were recorded at a frequency of once every 15 min throughout each sampling season (July, November 2018, February, and April 2019) by an automatic microclimatic station (Campbell Scientific, Inc., Logan, UT, USA). This station was installed in an open place within the study site with a distance of 250–2500 m away from the sampling plots (Fig. 1b) and an elevation of 5–25 m higher than the canopy. The accuracies of climate parameters were ±0.1 mm, 0.1 °C, 1%, and 0.1 MJm^{-2} for *P*, *T*, *RH*, and R_s, respectively. Meanwhile, the vapor pressure deficit (*VPD*, kPa) was calculated using *T* and *RH* per hour according to the following formula (Yang et al., 2015):

$$VPD = 0.611 \times Exp\left(\frac{17.502 \times T}{T + 24.97}\right) \times (1 - RH) \quad (4)$$

2.3. Measurement of sap flow

Sap flux density was determined based on the thermal diffusion

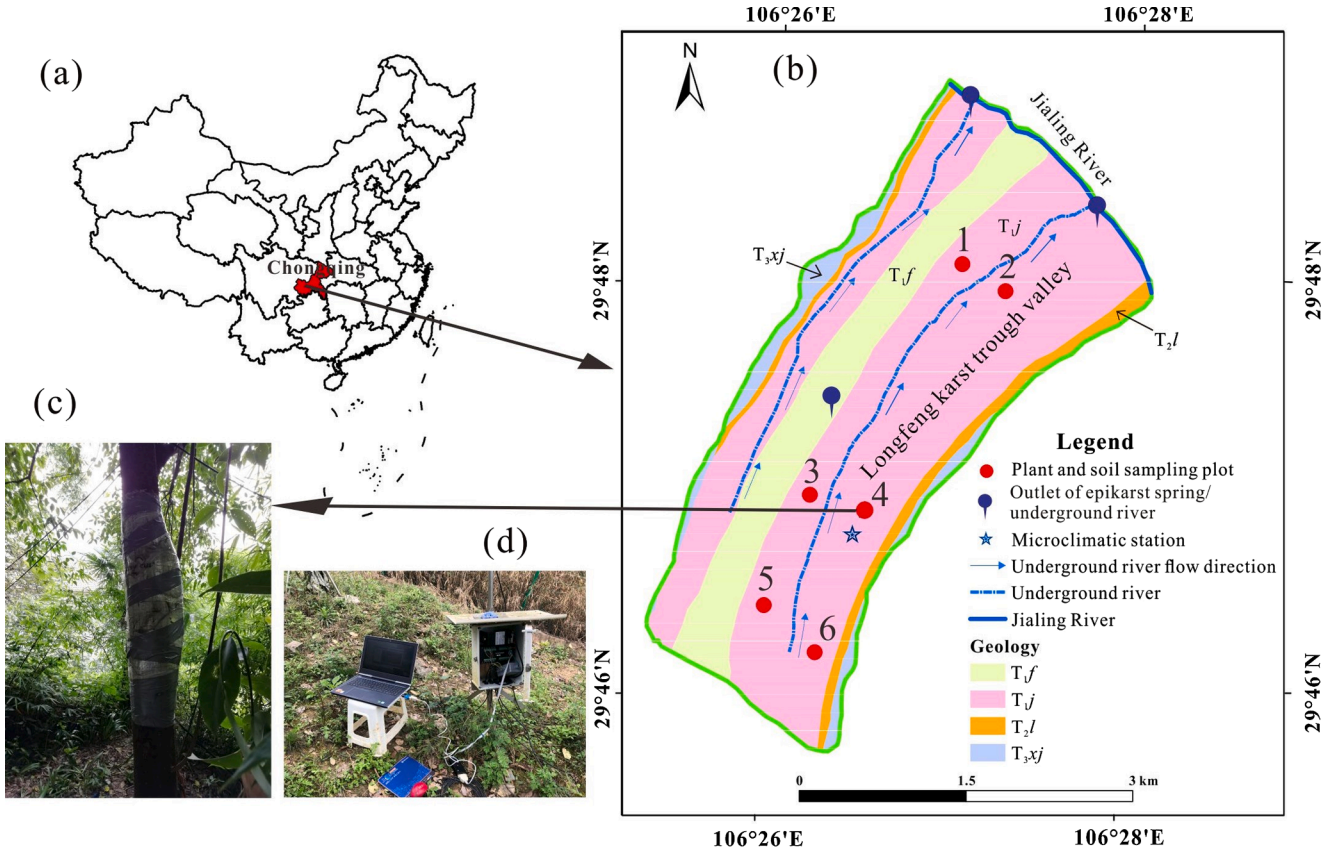

Fig. 1. (a) Geographic location of the study area; (b) Hydrological geology, and sampling points in the study area; (c) *Ligustrum lucidum*; (d) Sap flow measurement.

principle (Cohen et al., 1981; Burgess et al., 2001). For this, two replicate woody species of *Ligustrum lucidum* selected in the investigation plot 1 (Fig. 1b, c) were instrumented with thermal dissipation probes (Ecomatik, Germany)—installed on the north-facing side of plant stem (avoiding direct sunlight) at a height of 1.3 m with the distance of 10 cm between them (Fig. 1d). Measurements were performed every 30 s, and recorded as 15 averages, for 20 days from 5th to 25th day during each sampling season (July, November 2018, February, and April 2019). The measured *DBH* and sapwood area (mean ± 1 SD) were 13.1 ± 1.8 cm and 86.3 ± 19.4 cm^2, respectively. The instantaneous temperature difference between the probes was converted into a voltage value recorded by a data logger (DL2e, Delta-T Devices, UK). Sap flux density (*SFD*) of *Ligustrum lucidum* in the investigation plot was calculated according to the following formula (Granier, 1987):

$$SFD = 119 \times [(\Delta T_{max} - \Delta T)/\Delta T]^{1.231} \quad (5)$$

where *SFD* was sap flux density ($gH_2Om^{-2}\,s^{-1}$), ΔT was the temperature difference between the two probes (°C), and ΔT_{max} was the maximum value of ΔT recorded at the no-transpiration period when *SFD* was near zero (°C). To determine whole-tree transpiration, the obtained *SFD* data were normalized to minimize differences among replicated trees as described by Du et al. (2011).

Whole-tree daily transpiration (E_t, kgH_2Oday^{-1}) can be calculated by the equation:

$$E_t = \sum_t \left[A_s \times \left(\frac{SFD_{t_i} + SFD_{t_{i+1}}}{2} \right) \times 15 \times 60 \right] \Big/ 1000 \quad (6)$$

where A_s (m^2) is sapwood area, t_i is a time in a day, and the interval between t_i and t_{i+1} is 15 min; ×15 × 60 is time constant for s^{-1} converts to day^{-1}, /1000 is the constant for g converts to kg.

2.4. Plant tissue, soil, air, and water sample collection

Six 0.01 ha (10 × 10 m) plots that would cover almost the entire (spatial heterogeneity) study site were randomly established for plant and soil sampling (Fig. 1b). In each plot, a healthy mature woody species of *Ligustrum lucidum* (similar in diameter to the other selected trees) was selected for sampling in all seasons (July, November 2018, February, and April 2019). In each season, seven to ten leaves of each tree were collected using a pole pruner with no orientation when collecting them. Measurements were made using mature, intact, sunlit, upper canopy leaves. Then, all samples were dried in an oven at 70 °C for 3 days, frozen in liquid N_2 and ground to a powder (pass through a 100-mesh screen) for the $\delta^{13}C$ determination. Additionally, within each season, a 100-cm gas sample was collected using an air bag (300 mL) at the elevation (5–25 m) higher than that of all the sampling plots at the same meteorological station position—representing the air of the upper canopy—to measure the air CO_2 concentration for $\delta^{13}C_a$ determination (see Eqs. (7) and (8)). Moreover, three to five suberized branches of each tree were obtained from the canopy—branches were chipped in the field and immediately placed in a capped vial and wrapped in parafilm to minimize the effect of evaporative enrichment by water loss through unsuberized stems until extraction (Ehleringer & Dawson, 1992)—to analyze the δ^2H and $\delta^{18}O$.

At each plot, three spots were randomly chosen for soil sampling. Soil samples were collected with a soil auger from depths of 0–20 and 20–40 cm (n = 2 per soil layer) at each sampling season. All collected samples were immediately stored in the glass capped bottles, wrapped with parafilm to prevent the evaporation, and were kept frozen in a refrigerator until the δ^2H and $\delta^{18}O$ analysis. On the other hand, previous studies have shown (Liu et al., 2019; Cao et al., 2020) that the general trends in soil moisture (at depths of 0–20 and 0–40 cm) in multiple spots of the study site during different seasons were almost similar and there was no significant difference between sampling spots ($P > 0.05$). Therefore, we selected only one out of six sampling plots for a high-precision monitoring of soil moisture content (SMC, %). For this, two sensors (AV-EC5) were placed at the depth of 0–20 ($SMC_{0\text{-}20}$) and 20–40 cm soil ($SMC_{20\text{-}40}$) with the accuracy of ± 0.1%, and their SMC were continuously monitored by the RR-1016 data collector (Beijing Yugen Technology Co., Ltd., China) with a frequency of once every 15 min throughout each sampling season.

At each sampling season, a total of six deep-water (i.e., epikarst water and groundwater) samples were regularly gathered from the outlets of one epikarst spring (n = 2) and two underground rivers (n = 4) in the study site (Fig. 1b) for the $\delta^{18}O$ and δ^2H determination. All water samples collected were sealed and stored in the same manner as the plant (branches) and soil samples. All plant, soil, air, and water measurements were replicated with an interval of approximately 10–15 days within each season.

2.5. Isotopic analyses

Water was extracted from the *Ligustrum lucidum* (branches) stem and soil samples using a cryogenic vacuum distillation system (Ehleringer et al., 2000; Orlowski et al., 2013) (LI-2100, LICA, Beijing, China, extraction efficiency > 99%), transferred into 2-mL sealed brown bottles, and stored at 4 °C before conducting the δ^2H and $\delta^{18}O$ analyses. The δ^2H and $\delta^{18}O$ values were measured using a liquid water isotope analyzer (LWIA; GLA431-TLWIA (912–0050); Los Gatos Research, USA) at the National Monitoring Base for Purple Soil Fertility and Fertilizer Efficiency, Chongqing, China. To avoid errors of isotope ratios induced by organic compounds (Millar et al., 2018; West et al., 2010), the Spectral Contamination Identifier (LWIA-SCI) post-processing software (Los Gatos Research, Inc.) was employed to examine whether there was spectral interference in the isotope data from the extracted plant stem water, and corrected using the standard curves created by the Los Gatos Research engineers (Schultz et al., 2011). The δ^2H-H_2O and $\delta^{18}O$-H_2O values were expressed as the per mil (‰) deviation from the Vienna Standard Mean Ocean Water (VSMOW, accuracy for δ^2H and $\delta^{18}O$: ±0.5‰ and ±0.2‰, respectively).

The $\delta^{13}C$ values of the leaves and air were determined through an elemental analyzer coupled to an isotope-ratio mass spectrometer (EA-IRMS, USA) at the State Key Laboratory of Environmental Geochemistry, Institute of Geochemistry, Chinese Academy of Sciences, Guiyang, China. The $\delta^{13}C$ values were expressed as the delta-notation per mil (‰) deviation from the standard Vienna Pee Dee Belemnite (V-PDB, accuracy: ±0.2‰).

2.6. Data analysis

The δ^2H and $\delta^{18}O$ values of xylem water can provide information on the water sources of plants (Jackson et al., 1999). Both epikarst spring and the underground river were considered as a deep-water source, because their water samples exhibited similar isotopic compositions and could be distinguished from other water sources, i.e., soil water from upper lower soil layers. We applied IsotopeR as a comprehensive Bayesian mixing model to calculate relative contribution of each water source to the stem water of the woody plant (the basic terms and formulas and prior distributions of the model with comparative analysis are presented by Hopkins & Ferguson, 2012). We first carried out several sensitivity analyses using the isotopic signatures (i.e., $\delta^{18}O$ and δ^2H) of mixture and source population to test the relative impact of (1) sample size, (2) isotopic signature standard deviations (SD) in the mixture and source populations, (3) the isotopic signature difference between the sources, (4) analytical SD (i.e., SD among replicated samples), and (5) the value of inferences for different sources so as to find situations where the uncertainty of source proportion estimates could be minimized (see e.g., Phillips & Gregg, 2001). Accordingly, we found that the population had a major effect on individual source estimates, so that increasing the sample size—especially when replicated measurements of the same

individual were included—significantly reduced the proportion variability (SD) and improved the inferences. Therefore, we extended our model with a shared individual variance across populations. It should be added that each individual had a unique mean and variance for each isotopic signature, which were assumed to follow independent normal distributions (Semmens et al., 2009). Besides, it was necessary to calculate an isotopic correlation coefficient for the mixtures and the sources to accurately estimate proportional source contributions, because the $\delta^{18}O$ and $\delta^{2}H$ signatures in individual plant and soil water compartments are often highly correlated (Phillips & Gregg, 2001). Therefore, we calculated these values using Bayesian methods to correct the variance estimates for all the sources and then incorporated those as terms in the covariance matrix. In addition to including these corrections, we accounted for the error associated with measurement and incorporated it to each observation in our model. However, we did not include a residual error term (to account for the uncertainty otherwise unaccounted for in the mixture and source populations) in our estimation process as the correlation in the mixture population was accounted for by the correlation in the sources (see e.g., Hopkins & Ferguson, 2012). Following Semmens et al. (2009), a Gibbs sampler (a Markov chain Monte Carlo algorithm) was applied to perform the model, with random effects to allow for individual variation within populations, using 3 parallel chains in JAGS. In the end, we reported our estimates as average (±1SD) for the individual sources at the population level (Fig. 4a).

Photosynthetic ^{13}C discrimination ($\Delta^{13}C$) was calculated from the $^{13}C/^{12}C$ ratio in leaves according to Farquhar and Richards (1984):

$$\Delta^{13}C = \frac{\delta^{13}C_a - \delta^{13}C_p}{1 + \delta^{13}C_p/1000} \quad (7)$$

where $\delta^{13}C_a$ and $\delta^{13}C_p$ were the $\delta^{13}C$ values of CO_2 in ambient air (assumed to be −8‰; Seibt et al., 2008) and plant leaves, respectively.

Intrinsic water use efficiency (WUE_i) was estimated using the species mean $\Delta^{13}C$ according to a leaf-scale model of C_3 photosynthetic isotope discrimination (Farquhar et al., 1989):

$$WUE_i = \frac{C_a(b - \Delta^{13}C)}{1.6(b - a)} \quad (8)$$

C_a was the CO_2 concentration in the ambient air, a was the $^{13}CO_2$ fractionation as a result of diffusion through stomata pores (4.4‰; O'Leary, 1981), and b was the fractionation during carboxylation by the CO_2-fixing enzyme Rubisco (27‰; Farquhar & Richards, 1984). Notably, this simplified linear model can also implicitly account for internal CO_2 transfer (Seibt et al., 2008), which often leads to the overestimation of $\Delta^{13}C$ (and thus underprediction of WUE_i), and this deviation is augmented with assimilation rate especially in plant growth period when there is a high rate of assimilation and photosynthesis (Farquhar et al., 1989). Therefore, we did take into account possible uncertainty associated with it, although our main focus was not to estimate the actual value of WUE_i.

Fitting of the model according to multiple linear regression and other statistical analyses were conducted using IBM SPSS Statistics 25 (IBM Co., NY, USA). It should be added that all variables in the regression analysis were standardized using a Enter method and standardized coefficients were interpreted.

3. Results

3.1. Seasonal variations in precipitation and air temperature

The total precipitation throughout the study period (July 2018–April 2019) was 823.6 mm, about 84% (692.1 mm) of which occurred between July and October 2018, and April 2019 (i.e., the rainy season) with the highest monthly precipitation amount occurring in July (199 mm). Most precipitation events during this period were relatively intense and frequent, which would result in lower stress for plant water uptake. Approximately, 16% of precipitation (131.5 mm) occurred between November 2018 and March 2019 (dry season), with the lowest monthly precipitation amount occurring in February 2019 (3.9 mm; Fig. 2a). Most precipitation events during this five-month period were less intense with lower frequency, which may increase the water stress on plants, driving them to obtain water from different sources (Cao et al., 2020).

The monthly average estimated mean, minimum, and maximum temperatures throughout the study period were 19.5, 7.1, and 36.6 °C, respectively. The highest and lowest monthly average daily temperatures recorded were 32.3 and 11.1 °C in July 2018 and February 2019, respectively (Fig. 2a).

3.2. Seasonal variations in soil moisture content

As shown in Fig. 2b, there were significant differences in the soil moisture content (SMC) of the upper and lower soil layers ($P < 0.05$), with average values of 23.4 and 28.5%, throughout the study period (July 2018–April 2019), respectively, indicating that in the lower soil layer there was always—during the different seasons—more moisture content for plant uptake. In addition, there were significant temporal changes in the SMC of both soil layers that were consistent with the seasonal variations in precipitation. The average SMC of the upper and lower soil layers were 32.3 and 26.1% during the rainy season, and 24.7 and 20.7% during the dry season, respectively. This indicates a significant reduction in the SMC of the soil layers due to the remarkable reduction in rainfall, which could cause severe stress in plants when taking up water from the soil layers.

Fig. 2 Daily variations in (a) precipitation (P; mm), air temperature (T; °C); (b) soil moisture content (%) at depths of 0–20 cm ($SMC_{0\text{-}20}$) and 20–40 cm ($SMC_{20\text{-}40}$); (c) vapor pressure deficit (VPD) and net radiation (Rs; MJm^{-2}); and (d) tree transpiration (*Et*; kgH_2Oday^{-1}). Data of *Et* was average of two replicate tree species of *Ligustrum lucidum*.

3.3. Seasonal variations of transpiration (Et)

The E_t results indicated that there were significant seasonal variations in the plant water uptake ($P < 0.05$; Fig. 2d). The average daily E_t of *Ligustrum lucidum* in July and November 2018, and February and April 2019 were 15.5 (varying from 5.2 to 22.9 kg H_2O day^{-1}), 1.6 (varying from 0.7 to 3.2 kg H_2O day^{-1}), 1.8 (varying from 0.9 to 3.8 kg H_2O day^{-1}), and 6.8 kgH_2Oday^{-1} (varying from 1.9 to 10 kg H_2O day^{-1}), respectively. Accordingly, the average proportions of plant water uptake occurring in July and November 2018, and February and April 2019 were 60, 6, 7, and 27%, respectively. These results indicated that the amount of plant water uptake during the rainy (growing) season (especially in July 2018) was significantly higher than that during the dry season. Based on the standard multiple linear regression models presented below, both the rainy and dry seasons, the variations in E_t were affected by six environmental factors including air temperature (T), VPD, R_s, precipitation (P), upper soil moisture ($SMC_{0\text{-}20}$), lower soil moisture ($SMC_{20\text{-}40}$):

$$E_t = 0.78T - 0.13P + 0.09R_s + 0.80VPD + 0.06SMC_{0-20} + 0.38SMC_{20-40} \quad (Rainy\ season; R^2 = 0.82, P < 0.001) \quad (9)$$

$$E_t = -0.14T + 0.09P + 0.37R_s + 0.82VPD + 0.04SMC_{0-20} - 0.05SMC_{20-40} \quad (Dry\ season; R^2 = 0.83, P < 0.001) \quad (10)$$

According to our results, during the rainy season, the contribution of each explanatory variable to the E_t was highly statistically significant (Eq. (9); t-test, $P < 0.05$, Table 1), so that E_t was affected more by VPD, T, and $SMC_{20\text{-}40}$, respectively (Eq. (9); $P < 0.001$). In contrast, none of them significantly affected E_t during the dry season (Eq. (10); $P > 0.1$), excluding R_s and VPD (Eq. (10); $P = 0.022$ and $P < 0.001$, respectively).

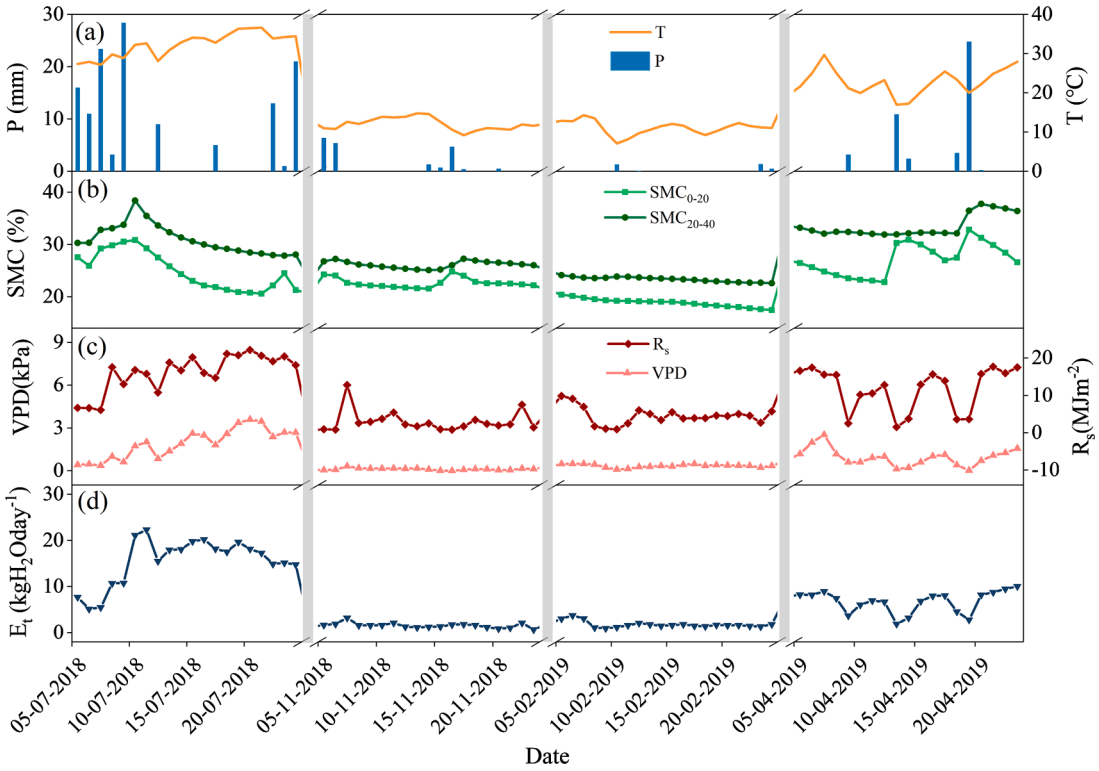

Fig. 2. Daily variations in (a) precipitation (P; mm), air temperature (T; °C); (b) soil moisture content (%) at depths of 0–20 cm ($SMC_{0\text{-}20}$) and 20–40 cm ($SMC_{20\text{-}40}$); (c) vapor pressure deficit (VPD) and net radiation (Rs; MJm^{-2}); and (d) tree transpiration (*Et*; kgH_2Oday^{-1}). Data of *Et* was average of two replicate tree species of *Ligustrum lucidum*.

Table 1
Statistically significant comparison (using *t*-test) between daily transpiration (*Et*) of *Ligustrum lucidum* and influential environmental factors during the rainy and dry seasons of 2018–2019.

	Rainy season		Dry season	
Environmental factors	*t*	*sig*	*t*	*sig*
T	5.434	<0.001	−1.667	0.105
P	−2.067	0.002	0.904	0.372
R_s	1.994	0.007	2.413	0.022
VPD	6.625	<0.001	7.763	<0.001
$SMC_{0\text{-}20}$	1.201	0.044	0.170	0.484
$SMC_{20\text{-}40}$	3.480	<0.001	−0.265	0.460

T: air temperature (°C), *P*: precipitation (mm), R_s: net radiation (MJm^{-2}), *VPD*: vapor pressure deficit (kPa), $SMC_{0\text{-}20;\ 20\text{-}40}$: soil moisture content (%) at depths of 0–20 and 20–40 cm.

Remarkably, the sensitivity of E_t to soil moisture in both soil layers, as the potential source water of plant, was significant only during the rainy (Eq. (9); $P < 0.05$).

3.4. Seasonal variations of stable isotopes (δ^2H and $\delta^{18}O$) and water sources

The δ^2H and $\delta^{18}O$ values of the xylem water samples were significantly more positive during the dry season (November 2018 and February 2019) than those during the rainy season (July 2018 and April 2019; Fig. 3a, b; Table 2). The δ^2H values of the xylem water samples in July and November 2018, and February and April 2019 were −69.8, −47.4, −45.2, and −52.8‰, respectively (Table 2), with an average value of −53.8‰, and their $\delta^{18}O$ values were −9.8, −7.5, −8.2, and −8.4‰, respectively, with an average value of −8.5‰. The isotopic values (δ^2H and $\delta^{18}O$) of the soil water varied seasonally and with soil depth at the study area, and the δ^2H and $\delta^{18}O$ values of the soil water samples from both soil layers were more positive during the dry season (November 2018 and February 2019) than those during the rainy season (July 2018 and April 2019) (Fig. 3a, 3b; Table 2).

However, the δ^2H and $\delta^{18}O$ values of soil water samples for the upper soil layer were more positive than those of the lower soil layer. The δ^2H values of the soil water samples of the upper soil layer in July and November 2018, and February and April 2019 were −77.4, −46.9, −40.4, and −53.3‰ respectively (Table 2), with an average value equal of −54.5‰, and their $\delta^{18}O$ values were −9.3, −7.4, −7.3, and −9.0‰ respectively (Table 2), with an average value equal of −8.2‰. In contrast, the δ^2H values for the soil water samples from the lower soil layer in July and November 2018, and February and April 2019 were -80.1, −52.2, −48.6, and −64.5‰, respectively, with an average value of −61.4‰, and the $\delta^{18}O$ values were −10.7, −8.1, −8.5, and −10.4‰ respectively, with an average value equal of −9.4‰. The δ^2H and $\delta^{18}O$ values of deep-water (epikarst water and groundwater) samples during the rainy season were close to those during the dry season and varied less than those of the soil water samples. The δ^2H values of the deep-water samples in July and November 2018, and February and April 2019, were -53.0, −45.3, −44.8, and −43.6‰, respectively (Table 2), with an average value equal of −46.7‰, and their $\delta^{18}O$ values were −8.8, −7.3, −8.3, and −6.9‰, respectively (Table 2), with an average value equal of −7.8‰. These small variations in the δ^2H and $\delta^{18}O$ values of the deep water during the study period agreed with the results reported in other studies (Perrin et al., 2003; McCole and Stern, 2007; Nie et al., 2012).

Fig. 3 Temporal variations in the values of (a) δ^2H and (b) $\delta^{18}O$ in plant xylem, upper soil, lower soil, and deep-water samples, and (c) plant leaf $\delta^{13}C$ during different seasons (2018–2019). All data were presented as average ± 1SD of replicates.

The IsotopeR mixing model was used to determine the proportions of various water sources used by *Ligustrum lucidum*. According to the IsotopeR outputs, there were significant seasonal variations in the

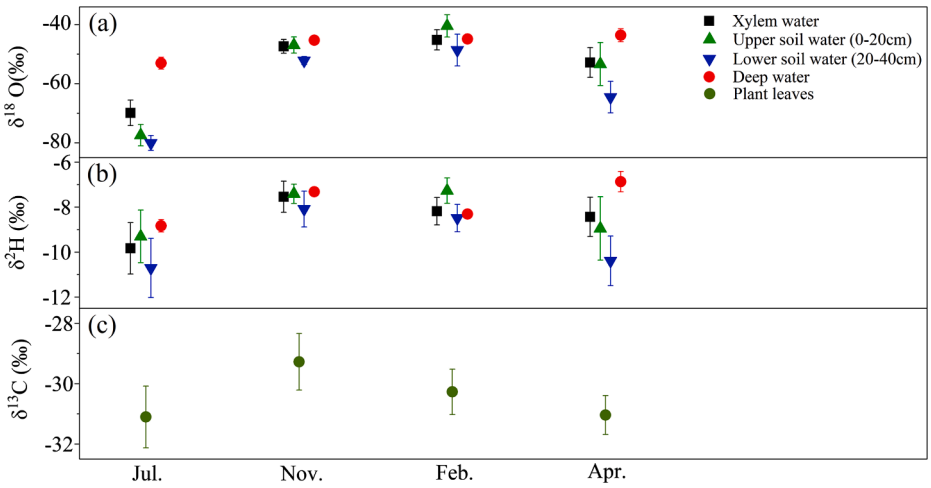

Fig. 3. Temporal variations in the values of (a) $\delta^{2}H$ and (b) $\delta^{18}O$ in plant xylem, upper soil, lower soil, and deep-water samples, and (c) plant leaf $\delta^{13}C$ during different seasons (2018–2019). All data were presented as average ± 1SD of replicates.

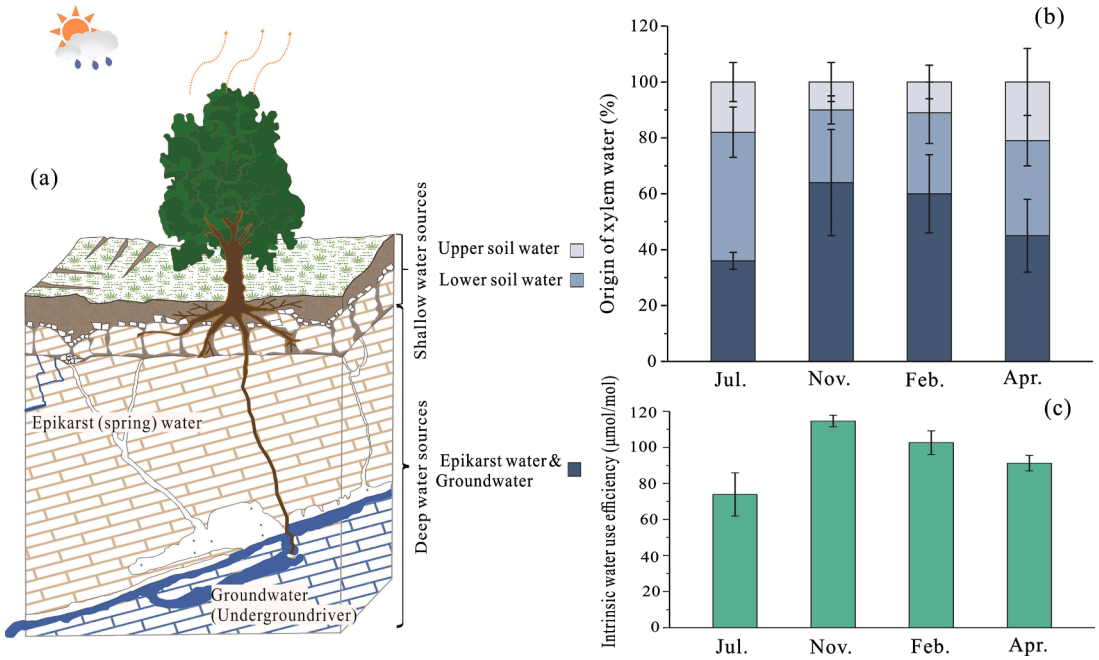

Fig. 4. (a) Conceptual diagram of water source pools available for an endemic woody plant species (*Ligustrum lucidum*) in a limestone karst area; (b) Proportions (%) of the contributions of potential water sources (upper and lower soil water, and deep water) used by *Ligustrum lucidum*; and (c) intrinsic water use efficiency (WUE_i) values of the woody plant during different seasons (2018–2019). All results were presented as average ± 1SD of replicates.

proportions of the various water sources for plant uptake (Fig. 4b). In July 2018 (mid-rainy season), *Ligustrum lucidum* mostly utilized water from the lower soil layer (average (±1SD) proportions of 46 ± 9%), followed by the deep-water pools (i.e., epikarsts and underground river) and upper soil layer (average proportion of 36 ± 3% and 18 ± 7%, respectively). In November 2018 and February 2019 (early to mid-dry season), the plant primarily extracted water from the deep-water pools (average proportions of 64 ± 19% and 60 ± 14%, respectively), followed by the lower (average proportions of 26 ± 5% and 29 ± 11%, respectively) and upper (average proportions of 10 ± 7% and 11 ± 6%, respectively) soil layers. In April 2019 (early rainy season), the plant mostly utilized water from the the deep-water pools (average proportion of 45 ± 13%), followed by that from the lower and upper soil layers (average proportions of 34 ± 9% and 21 ± 12%, respectively).

3.5. Seasonal variations of leaf $\delta^{13}C$ values and WUEi

The mean leaf $\delta^{13}C$ and WUE_i values of *Ligustrum lucidum* varied significantly between the rainy and dry seasons (Figs. 3c, 4c; Table 3). The mean $\delta^{13}C$ values of *Ligustrum lucidum* leaves in July and November 2018, and February and April 2019 were −31.10, −29.27, −30.27, and −31.04‰, respectively, with an average value of −30.42‰ (Fig. 3c; Table 3). However, the mean WUE_i values of *Ligustrum lucidum* in July and November 2018, and February and April 2019 were 73.91, 114.59, 102.58, and 91.22 μmol/mol, respectively, with an average value of 95.58 μmol/mol (Fig. 3c; Table 3). The smallest $\delta^{13}C$ and largest WUE_i occurred in July 2018 (mid-rainy season), with average values of −31.10‰ and 73.91 μmol/mol, respectively, and the largest discrimination and the smallest WUE_i occurred in November 2018 (early dry season), with average values of −29.27‰ and 114.59 μmol/mol,

Table 2
δ^2H and $\delta^{18}O$ values of soil (different soil layers), deep (epikarst spring and underground river), and plant xylem water samples during different seasons (2018–2019).

Water sources		July 2018		November 2018		February 2019		April 2019	
		δ^2H (‰)	$\delta^{18}O$ (‰)	δ^2H (‰)	$\delta^{18}O$ (‰)	δ^2H (‰)	$\delta^{18}O$ (‰)	δ^2H (‰)	$\delta^{18}O$ (‰)
Xylem water (n = 6)	min	−74.96	−11.87	−50.44	−8.44	−49.83	−8.95	−62.83	−9.82
	max	−61.80	−7.95	−43.12	−6.20	−39.39	−7.14	−46.79	−7.14
	mean	−69.84	−9.83	−47.35	−7.54	−45.15	−8.18	−52.81	−8.43
Upper soil water (n = 6)	min	−82.85	−11.24	−50.89	−7.95	−45.74	−8.20	−65.19	−11.29
	max	−70.79	−7.95	−42.08	−6.66	–33.78	−6.32	−44.84	−6.26
	mean	−77.40	−9.30	−46.88	−7.41	−40.42	−7.26	−53.33	−8.95
Lower soil water (n = 6)	min	−84.77	−12.23	−53.96	−9.58	−58.10	−9.18	−71.15	−11.64
	max	−76.72	−9.05	−50.15	−7.08	−39.59	−7.24	−53.92	−7.95
	mean	−80.05	−10.71	−52.18	−8.08	−48.63	−8.49	−64.52	−10.39
Deep water (n = 3)	min	−55.80	−9.09	−45.82	−7.36	−46.63	−8.58	−46.71	−7.47
	max	−51.26	−8.45	−44.63	−7.26	−43.27	−8.13	−41.77	−6.37
	mean	−53.03	−8.83	−45.28	−7.32	−44.84	−8.31	−43.59	−6.87

All data were averages of replicates.

Table 3
Leaf $\delta^{13}C$ and WUE_i values of *Ligustrum lucidum* during different seasons (2018–2019).

	July 2018		November 2018		February 2019		April 2019	
	$\delta^{13}C$ (‰)	WUE_i (μmol/mol)	$\delta^{13}C$ (‰)	WUE_i (μmol/mol)	$\delta^{13}C$ (‰)	WUE_i (μmol/mol)	$\delta^{13}C$ (‰)	WUE_i (μmol/mol)
min	−32.20	54.98	−30.21	111.37	−31.33	93.74	−32.11	83.75
max	−29.97	88.26	−28.33	117.81	−29.30	111.73	−30.19	96.33
mean	−31.10	73.91	−29.27	114.59	−30.27	102.58	−31.04	91.22

All results were averages of replicates.

respectively.

4. Discussion

4.1. Ecological significance of seasonal transpiration and its relationship with key environmental factors

Our results showed that the plant water use rate significantly varied from one season to another. Accordingly, the plant taken up a remarkable amount of water (approximately 87% of its total annual transpiration) during the rainy (growing) season (particularly during the middle of the rainy season, July 2018) while it did much less during the dry season. The high rate of transpiration was very important during the growing season, as previous studies had also emphasized, as it could mainly contribute to photosynthesis and plant growth (Oren and Pataki, 2001; Yepez et al., 2003; Scott et al., 2006; Cavanaugh et al., 2011). Besides, some studies have also shown that a small amount of transpiration during each dry season has been required to maintain the plant health and functioning until the next growing season (Biederman et al., 2018; Szutu & Papuga, 2019).

According to the results, several potential reasons might have explained the high rate of water use during the rainy season, the most popular of which was an increase in *VPD* (frequently exceeding 1 kPa; Fig. 2c), resulting in more stomatal conductance and further escape of water molecules from plant leaves to form transpiration (Fetcher et al., 1994; Zheng & Wang, 2014). The increase in *T* (Fig. 2a) was another significant factor, as it would primarily enhance photosynthetic production and the plant growth (Hari et al., 1986; Nöjda et al., 2017). We also found that the transpiration of the plant was sensitive to soil moisture in both soil layers (especially lower soil layer), as the soil moisture was the predominant source of the plant water uptake during the rainy season which would regularly replenish by significant rainfall with relatively high frequency, keeping soil drought stress to a minimum. However, as we will explain in the next section, soil moisture alone was not enough to supply all the water needed to be transpired by the plant during the rainy season, and the rest (on average 41%) would come from deep-water source pools. Overall, these findings were in line with some previous studies, which have shown that higher *VPD* and T at moist sites during growing season (when ample water is available to the plant water uptake) increase transpiration dynamics (Xu & Li, 2006; Clausnitzer et al., 2011; Zheng & Wang, 2014; Yan et al., 2018). In contrast, low transpiration during the dry season was the result of *VPD* rarely exceeding 1 kPa with R_s (Fig. 2c), implying a strong stomatal control facing water stress (Schulze et al., 1994; Yan et al., 2018). Additionally, it could be associated with a significant reduction in soil moisture due to a significant reduction in rainfall during the dry season, as our results indicated that transpiration was not sensitive to any moisture in the two soil layers during this period time—primarily because the plant extracted a significant fraction of little water required for its dry season transpiration from deep-water source pools (explained in the next section). Secondly (and most importantly), due to a strong stomatal control linked to limited available soil moisture, as water stress has been found to increase the sensitivity of canopy stomatal control or plant hydraulic resistance to light and vapor pressure deficit during the drought periods (Zheng & Wang, 2014; Wang et al., 2020), decreasing the water use from deep-water source pools even if there was ample water in those pools to absorb. Similar findings have also been reported from previous studies that there is a significant relationship between drought sensitivity and the relative reduction in the amount of water used by drought-sensitive tree species during dry periods, which has been associated with the deficit of soil moisture due to low and insufficient amount of rainfall (Sperry et al., 2002; Du et al., 2011; Chang et al., 2014; Nan et al., 2019). Accordingly, the endemic woody plant species of *Ligustrum lucidum* can be categorized as drought-sensitive, because its transpiration rate was significantly influenced by the seasonal variations in rainfall and soil moisture (Du et al., 2011; Yan et al., 2018).

4.2. The nature of seasonal water sources transpired by Ligustrum lucidum

The results showed that *Ligustrum lucidum* utilized a combination of all of the potential water sources during all seasons; thus, during the rainy season (July 2018 and April 2019), when the water stress was low

(and soil moisture content was high) due to the sufficient rainfall capture by the soil layers, this tree species predominantly utilized the soil water, and used less deep water (epikarst water and groundwater) than it did during the dry season (November 2018 and February 2019). In contrast, during the dry season, the fraction of deep water in the xylem water of *Ligustrum lucidum* increased significantly with increasing water stress and decreasing soil moisture content due to the low rainfall and water holding capacity in the shallow soils of this heterogeneous karst area. This indicates a clear seasonal shift in the water-use strategy of *Ligustrum lucidum*. Moreover, it could also be a clear indicator of specialized (dimorphic) root systems for the plant allowing to extract water from shallow water sources (growth pools) during the rainy season and from deep-water sources (maintenance pools) during the dry season (Ryel et al., 2008, 2010). Some studies in karst areas with shallow soils have documented that the roots of plants are predominantly restricted to the upper 2 m of the soil/bedrock profile (Querejeta et al., 2007; Hasselquist et al., 2010). Therefore, it could be difficult for the plant to develop most of its shallow roots deep into the lower layers of the bedrock. However, several studies have reported that the roots of many plants in limestone karst areas with shallow soils can grow deep into the lower layers of the bedrock (White et al., 1985; Jackson et al., 1999; Querejeta et al., 2006, 2007; Schwinning, 2008; Nie et al., 2011; Estrada-Medina et al., 2013; Heilman et al., 2014; Liu et al., 2019; Carrière et al., 2020). Recently, Liu et al. (2019) reported similar seasonal water-use strategies for two other native tree species in the same area, implying flexibility in gaining access to shallow and deep-water source pools during different seasons in this heterogeneous karst area to compensate for limited soil water storage, particularly during the dry season. The water-use strategies due to changing environmental conditions are referred to as "plasticity dimorphic root systems" (Liu et al., 2014). Furthermore, the analysis of the IsotopeR results indicated that, despite the permanent and reliable access to deep-water source pools in the rainy season, providing more water storage for plant uptake than what was available in dry season, *Ligustrum lucidum* tended to use more of shallow water pools. As we will explain in the next section, this could likely be due to the fact that taking up water from deep-water source pools by deep root systems requires more metabolic energy compared to the water that is captured by shallow root systems (Ksenzhek & Volkov, 1998). Some recent studies have also demonstrated that plants use deep-water source pools only to maintain their growth and survival under drought stress conditions, even when the pools can provide large amounts water for plant uptake (Ryel et al., 2008, 2010). Bleby et al. (2010) documented that deep roots (depth of 20 m) were approximately five times more active than the shallow roots (depth of 0–0.5 m) during drought periods when the shallow water supply was insufficient for plant use; however, after receiving rainfall and balancing shallow water storage, the deep roots were immediately deactivated. Therefore, *Ligustrum lucidum* used shallow water source pools as an energy-efficient options for supporting growth, and used deep-water source pools as energy-demanding but safe options only for maintaining their survival. Water source pools as well as their proportion contributions of used by *Ligustrum lucidum* were presented to compare in a conceptual model (Fig. 4a, b).

Fig. 4(a) Conceptual diagram of water source pools available for an endemic woody plant species (*Ligustrum lucidum*) in a limestone karst area; (b) Proportions (%) of the contributions of potential water sources (upper and lower soil water, and deep water) used by *Ligustrum lucidum*; and (c) intrinsic water use efficiency (WUE_i) values of the woody plant during different seasons (2018–2019). All results were presented as average ± 1SD of replicates.

4.3. Relationship between transpiration with WUE_i and elucidation of seasonal ecohydrological events

According to the results, the *Ligustrum lucidum* leaf $\delta^{13}C$ values ranged from −28.33 to −32.20‰ similar to those of other dominant tree species in the same area (−28.1 to −32.8‰; Cao et al., 2020), indicating that the photosynthetic pathway of this tree species belongs to C_3 plants, whose leaf $\delta^{13}C$ values (−20 to −35‰) differ from those of C_4 plants (−7 to −15‰; O'Leary 1981). As our results showed, WUE_i (and $\delta^{13}C$) was low during the rainy season (Figs. 3c, 4c; Table 3), just when significant transpiration (87% of total annual transpiration) occurred. This implies a partial (plant's leaves) stomatal opening during this time period, facilitating the release of water molecules (in the form of unsaturated vapor) and the entry of CO_2 molecules through plant leaves (Ball et al., 1987; Collatz et al., 1991). As a result, these interactions could intensify the plant's thirst (Ainsworth & Rogers, 2007), hence prompting the plant to take up more water from the available water sources. Most researchers believe that the main role in the amount of water that can be taken up—and its translocation from the roots to the leaves—is related to transpiration, which provides the formation of a hydrodynamic pressure gradient along the entire length of a plant (due to the formation of negative pressure in its upper parts i.e., leaves), hence allowing to pull sap through the plant xylem vessels without the need to spend any metabolic energy (Ksenzhek & Volkov, 1998). Thus, the greater the intensity of transpiration, the greater the amount of water pulled along the xylem vessels. However, the action of pulling water caused by the hydrodynamic pressure gradient is not sufficient to stimulate the plant's transport systems because the plant effectively employs a special force called root pressure, capturing the water from the corresponding water source pools (soil water and deep water) through root systems and pumping it into the xylem vessels at the expense of a minimum metabolic energy (Ksenzhek & Volkov, 1998). As described above, during the rainy season, *Ligustrum lucidum* tended to obtain more water from the soil layers just when these water pools could be sufficiently fed by abundant rainfall with high frequency. This suggests that water extraction from these shallow water source pools would likely be more time-saving and energy-efficient for the plant use compared to the deep-water source pools, as shorter transport (from the shallow water pools) probably needed to generate less root pressure for delivering the water to the xylem. In addition to these physiological events, the entry of CO_2 which is recognized as an essential component in the process of photosynthesis (Collatz et al., 1991) could potentially help increase the rate of photosynthesis and plant growth (Ainsworth & Rogers, 2007). Thus, during the rainy season, minimum water stress associated with soil moisture deficit could occur and impact the normal plant water-uptake process, allowing the plant to maximize its growth and photosynthesis rates without reducing stomatal conductance and the transpiration rate. This suggests that *Ligustrum lucidum* might simultaneously benefit from profligate water-use strategy during the rainy season (Nie et al., 2014; Cao et al., 2020). Accordingly, under this water-use strategy, the water that the plant could easily (cheaply) obtain from soil layers through its shallow roots could also be easily (profligately) lost through its leaves during the rainy season. In contrast, during the dry season, the plant would suffer from a shortage of soil water due to a significant reduction in rainfall. According to our results, it seems that the plant adopted a constructive strategy for managing this water stress during the dry season (Yan et al., 2018; Wang et al., 2020), as it had increased its WUE_i by an average of 15% and reduced its total transpiration rate by approximately one-seventh of the rainy season transpiration (i.e., equivalent to 13% of its total annual transpiration). Thus, this sharp decrease in transpiration rate, reflecting the partial stomatal closure of the plant's leaves, limits the formation of a hydrodynamic pressure gradient, hence preventing the plant from taking up too much water from the available water source pools (Huc & Guehl, 1989; Granier et al., 1992). Additionally, given that most of its water needed during this time period comes from deep-water source pools (on average 62%), capturing and pumping (the same small amount) water by deep root systems required more energy than the (fraction) of water that could be extracted from the soil water pools and delivered to its xylem vessels (Ksenzhek & Volkov, 1998). However, despite having the necessary tool (dimorphic root system) to extract deep water, even if there was enough

water in these pools, the plant would be unable to lift much more water (along its xylem vessels) during the dry season for the same reason mentioned earlier (i.e., the existence of a limited hydrodynamic pressure gradient due to very low transpiration; Granier et al., 1992). As a result, this mechanism would not allow the plant to alleviate all of the drought stress associated with the soil moisture deficit by taking up enough (or more) water from deep-water source pools.

Overall, all of these ecohydrological events show that the plant tended to adopt a conservative water uptake strategy during the dry season. Consequently, the plant had to extract uneasily (expensively) most of the required water (albeit at a small amount) through deep-water source pools and consume it uneasily (conservatively) through increasing the WUE_i (by reducing its (leaves) stomata) in order to maintain its survival during the dry season.

5. Conclusions

We investigated transpiration responses and water-use strategies of a dominant evergreen tree species (*Ligustrum lucidum*) growing in a karst habitat with the typical shallow soils, which relies on various water sources. The site chosen was a subtropical (limestone) karst area on southwest China. To achieve our goals, we took into account seasonal variations in the sap flow transpiration rates, leaf $\delta^{13}C$, and $\delta^{2}H$ and $\delta^{18}O$ of the soil moisture (upper and lower soil layers), deep water (epikarst water and groundwater), and tree stem water samples. Using the sap flow and soil moisture data, we found that *Ligustrum lucidum* maintained its rainy (growth) season transpiration at high rates under the control of key environmental factors such as *VPD* and *T* in response to favorable soil moisture conditions. However, it reduced its dry season transpiration at very low rates under the control of *VPD* and R_s due to sensitivity to unfavorable soil moisture conditions. According to the results obtained from the IsotopeR model (based on the $\delta^{2}H$ and $\delta^{18}O$ values), it was revealed that during different seasons, the plant used a combination of soil water and deep water, so that the contribution of the water obtained from the soil water was higher than the deep water during the rainy season and vice versa during the dry season. The signal of a seasonal shift in the pattern of the plant water uptake among different seasons was mainly attributed to the functionally dimorphic root system of *Ligustrum lucidum*, reflecting a greater degree of ecological plasticity of the plants in karst ecosystems. Meanwhile, it highlights that the transpiration dynamics of *Ligustrum lucidum* was largely a function of soil moisture and deep water during the rainy and dry seasons, respectively. Using the seasonal patterns of WUE_i values (based on the $\delta^{13}C$ values), we found that the plant water use efficiency was low and high during the rainy and dry seasons, respectively, signaling a seasonal shift in the water-use strategy for the plant from a profligate water-use pattern in the rainy season to a conservative water-use pattern in the dry season. Thus, *Ligustrum lucidum* overall strategy for managing the water consumption was obtaining the water efficiently and consuming it profligately in order to maximize its growth and photosynthesis rate during the rainy (growing) season. In contrast, the plant had to extract the water using much energy and consume it conservatively in order to maintain its survival during the dry season. Thus, applying a combined approach to understand the strategies and mechanisms of water use by plants, especially in the heterogeneous karst areas can help us gain more insights partly rather than simply using the sap flow or isotopic techniques alone.

CRediT authorship contribution statement

Ze Wu: Conceptualization, Visualization, Methodology, Software, Writing - original draft, Writing - review & editing. **Hamid M. Behzad:** Conceptualization, Visualization, Methodology, Software, Writing - original draft, Writing - review & editing. **Qiufang He:** Resources, Methodology, Investigation. **Chao Wu:** Investigation. **Ying Bai:** Visualization. **Yongjun Jiang:** Project administration, Funding acquisition, Conceptualization, Methodology, Writing - review & editing.

Declaration of Competing Interest

The authors declare that they have no known competing financial interests or personal relationships that could have appeared to influence the work reported in this paper.

Acknowledgements

This research was supported by the National Key Research and Developmental Program of China (2016YFC0502306), the Chongqing Municipal Science and Technology Commission Fellowship Fund (CSTC2019yszx-jcyjX0002), the Karst Dynamics Laboratory, MNR and GZAR (KDL&Guangxi 202007).

References

Ainsworth, S., Rogers, A., 2007. The response of photosynthesis and stomatal conductance to rising [CO_2]: mechanisms and environmental interactions. Plant, Cell Environ. 30, 252–270.

Alarcón, J.J., Domingo, R., Green, S.R., Sánchez-Blanco, M.J., Rodrígue, P., Torrecillas, A., 2000. Sap flow as an indicator of transpiration and the water status of young apricot trees. Plant Soil 227, 77–85.

Ball, J.T., Woodrow, I.E., Berry, J.A., 1987. A model predicting stomatal conductance and its contribution to the control of photosynthesis under different environmental conditions. In: Biggins I (ed) Progress in Photosynthesis Research, vol. IV. Proc Int Congr Photosynthesis. Martinus Nihjoff, Dordrecht, 221–224.

Barbeta, A., Peñuelas, J., 2016. Sequence of plant responses to droughts of different timescales: lessons from holm oak (Quercus ilex) forests. Plant Ecol. Divers. 9 (4), 321–338.

Barbeta, A., Mejía-Chang, M., Ogaya, R., Voltas, J., Dawson, T.E., Peñuelas, J., 2015. The combined effects of a long-term experimental drought and an extreme drought on the use of plant-water sources in a Mediterranean forest. Glob. Chang. Biol. 21, 1213–1225.

Berry, Z.C., Looker, N., Holwerda, F., Ortiz-Colín, P., Martínez, T.G., Asbjornsen, H., Rodrigo, L., 2017. Why size matters: the interactive influences of tree diameter distribution and sap flow parameters on upscaled transpiration. Tree Physiol. 10, 124.

Biederman, J.A., Scott, R.L., Arnone, J.A., Jasoni, R.L., Litvak, M.E., Moreo, M.T., et al., 2018. Shrubland carbon sink depends upon winter water availability in the warm deserts of North America. Agric. For. Meteorol. 249, 407–419.

Bleby, T.M., Mcelrone, A.J., Jackson, R.B., 2010. Water uptake and hydraulic redistribution across large woody root systems to 20 m depth. Plant. Cell Environ. 33, 2132–2148.

Burgess, S.S.O., Adams, M.A., Turner, N.C., Beverly, C.R., Ong, C.K., Khan., A.A.H., Bleby T.M., 2001. An improved heat pulse method to measure low and reverse rates of sap flow in woody plants. Tree Physiol 21, 589–598.

Cao, M., Wu, C., Liu, J., Jiang, Y., 2020. Increasing leaf $\delta^{13}C$ values of woody plants in response to water stress induced by tunnel excavation in a karst trough valley: implication for improving water-use efficiency. J. Hydrol. 586, 1–7.

Carrière, S.D., Martin-StPaul, N.K., Cakpo, C.B., Patris, N., Gillon, M., Chalikakis, K., Doussan, C., Olioso, A., Babic, M., Jouineau, A., Simioni, G., Davi, H., 2020. The role of deep vadose zone water in tree transpiration during drought periods in karst settings- insights from isotopic tracing and leaf water potential. Sci. Total Environ. 699, 134332.

Cavanaugh, M.L., Kurc, S.A., Scott, R.L., 2011. Evapotranspiration partitioning in semiarid shrubland ecosystems: a two-site evaluation of soil moisture control on transpiration. Ecohydrology 4 (5), 671–681.

Cernusak, L.A., Ubierna, N., Winter, K., JaM, H., Marshall, J.D., Farquhar, G.D., 2013. Environmental and physiological determinants of carbon isotope discrimination in terrestrial plants. New Phytol. 200, 950–965.

Chang, X.X., Zhao, W.Z., Liu, H., Wei, X., Liu, B., He, Z.B., 2014. Qinghai spruce (*picea crassifolia*) forest transpiration and canopy conductance in the upper Heihe river basin of arid northwestern china. Agric. For. Meteorol. 198–199, 209–220.

Chaves, M.M., Osorio, J., Pereira, J.S., 2004. Water Use Efficiency and Photosynthesis. CRC Press, Boca Raton, FL, pp. 42–74.

Clausnitzer, F., Köstner, B., Schwärzel, K., Bernhofer, C., 2011. Relationships between canopy transpiration, atmospheric conditions and soil water availability—analyses of long-term sap-flflow measurements in an old Norway spruce forest at the Ore Mountains/Germany. Agric. Forest Meteorol. 151 (8), 1023–1034.

Cohen, Y., Fuchs, M., Green, G., 1981. Improvement of the heat pulse method for determining sap flow in trees. Plant Cell Environ. 4, 391–397.

Collatz, G.J., Ball, J.T., Grivet, C., Berry, J.A., 1991. Physiological and environmental regulation of stomatal conductance, photosynthesis and transpiration: a model that includes a laminar boundary layer. Agric. For. Meteorol. 54, 107–136.

Craven, D., Hall, J.S., Ashton, M.S., Berlyn, G.P., 2013. Water-use efficiency and whole-plant performance of nine tropical tree species at two sites with contrasting water availability in Panama. Trees Struct. Funct. 27, 639–653.

Dawson, T.E., Mambelli, S., Plamboeck, A.H., Templer, P.H., Tu, K.P., 2002. Stable isotopes in plant ecology. Annu. Rev. Ecol. Syst. 33 (1), 507–559.

Ding, Y.L., Nie, Y.P., Chen, H.S., Wang, K.L., Querejeta, J.I., 2020. Water uptake depth is coordinated with leaf water potential, water-use efficiency and drought vulnerability in karst vegetation. New Phytol. 1–15.
Du, S., Wang, Y.L., Kume, T., Zhang, J.G., Otsuki, K., Yamanaka, N., Liu, G.B., 2011. Sapflow characteristics and climatic responses in three forest species in the semiarid Loess Plateau region of China. Agric. For. Meteorol. 151, 1–10.
Ehleringer, J.R., Dawson, T.E., 1992. Water uptake by plants: perspectives from stable isotope composition. Plant Cell Environ. 15 (9), 1073–1082.
Ehleringer, J.R., Roden, J., Dawson, T.E., 2000. Assessing ecosystem-level water relations through stable isotope ratio analyses. In: Sala, O.E., Jackson, R., Mooney, H.A., Howarth, R. (Eds.), Methods in Ecosystem Science. Springer, New York, pp. 181–198.
Esmaeilpour, A., Van Labeke, M.-C., Samson, R., Boeckx, P., Van Damme, P., 2016. Variation in biochemical characteristics, water status, stomata features, leaf carbon isotope composition and its relationship to water use efficiency in pistachio (*Pistacia vera L.*) cultivars under drought stress condition. Sci. Hortic. 211, 158–166.
Estrada-Medina, H., Graham, R.C., Allen, M.F., Jimenez-Osornio, J.J., Robles-Casolco, S., 2013. The importance of limestone bedrock and dissolution karst features on tree root distribution in northern Yucatan, Mexico. Plant Soil 362, 37–50.
Evaristo, J., Mcdonnell, J.J., Scholl, M.A., Bruijnzeel, L.A., Chun, K.P., 2016. Insights into plant water uptake from xylem-water isotope measurements in two tropical catchments with contrasting moisture conditions. Hydrol. Process 30 (18), 3210–3227.
Evaristo, J., McDonnell, J.J., Clemens, J., 2017. Plant source water apportionment using stable isotopes: a comparison of simple linear, two-compartment mixing model approaches. Hydrol. Process. 31 (21), 3750–3758.
Farquhar, G.D., O'Leary, M.H., Berry, J.A., 1982. On the relationship between carbon isotope discrimination and the intercellular carbon dioxide concentration in leaves. Aust. J. Plant Physiol. 9, 121–137.
Farquhar, G.D., Richards, R.A., 1984. Isotopic composition of plant carbon correlates with water use efficiency of wheat genotypes. Aust. J. Plant Physiol. 11, 539–552.
Farquhar, G.D., Ehleringer, J.R., Hubick, K.T., 1989. Carbon isotope discrimination and photosynthesis. Annu. Rev. Plant Biol. 40, 503–537.
Fetcher, N., Oberbauer, S.F., Chazdon, R.L., 1994. Physiological ecology of trees, shrubs, and herbs at La Selva. In: McDade, L.A., Bawa, K.S., Hespenheide, H.A., Hartshorn, G.S. (Eds.), La Selva: Ecology and Natural History of a Neotropical Rainforest. University of Chicago Press, Chicago, IL, USA, pp. 128–141.
Ford, D.C., Williams, P.W., 2007. Karst Hydrogeology and Geomorphology. Wiley, Chichester.
Granier, A., 1987. Evaluation of transpiration in a Douglas-fir stand by means of sap flow measurements. Tree Physiol. 3, 309–320.
Granier, A., Huc, R., Colin, F., 1992. Transpiration and Stomatal Conductance of Two Rain Forest Species Growing in Plantations (Simarouba amara and Goupia glabra) in French Guyana; Ann Sci For; EDP Sciences: Les Ulis, France.
Greco, S., Baldocchi, D.D., 1996. Seasonal variations of CO_2 and water vapour exchange rates over a temperate deciduous forest. Global Change Biol. 2, 183–197.
Han, C., Chen, N., Zhang, C., Liu, Y., Khan, S., Lu, K., Li, Y., Dong, X., Zhao, C., 2019. Sap flow and responses to meteorological about the Larix principis-rupprechtii plantation in Gansu Xinlong mountain, northwestern china. Forest Ecol. Manag. 451, 117519.
Hari, P., Raunemaa, T., Hautojärvi, A., 1986. The effects on forest growth of air pollution from energy production. Atmos. Environ. 20 (1), 129–137.
Hasselquist, N.J., Allen, M.F., Santiago, L.S., 2010. Water relations of evergreen and drought-deciduous trees along a seasonally dry tropical forest chronosequence. Oecologia 164 (4), 881–890.
Heilman, J.L., Litvak, M.E., McInnes, K.J., Kjelgaard, J.F., Kamps, R.H., Schwinning, S., 2014. Water-storage capacity controls energy partitioning and water use in karst ecosystems on the Edwards Plateau, Texas. Ecohydrology 7 (1), 127–138.
Hopkins III, J.B., Ferguson, J.M., 2012. Estimating the diets of animals using stable isotopes and a comprehensive Bayesian Mixing Model. PLoS One 7 (1), e28478.
Hu, Y., Zhao, P., Zhu, L., Zhao, X., Ni, G., Ouyang, L., Schäfer, K.V.R., Shen, W., 2019. Responses of sap flux and intrinsic water use efficiency to canopy and understory nitrogen addition in a temperate broadleaved deciduous forest. Sci. Total Environ. 648, 325–336.
Huang, Y., Li, X., Zhang, Z., He, C., Zhao, P., You, Y., MO, L., 2011. Seasonal changes in Cyclobalanopsis glauca transpiration and canopy stomatal conductance and their dependence on subterranean water and climatic factors in rocky karst terrain. J. Hydrol. 402(1-2), 135-143.
Huang, Y.Q., Zhao, P., Zhang, Z.F., Li, X.K., He, C.X., Zhang, R.Q., 2009. Transpiration of Cyclobalanopsis glauca (syn. Quercus glauca) stand measured by sap-flow method in a karst rocky terrain during dry season. Ecol. Res. 24, 791–801.
Huc, R., Guehl, J.M., 1989. Environmental control of CO2 assimilation rate and leaf conductance in two species of the tropical rain forest of French Guiana (Jacaranda copaia D.Don and Eperua falcata Aubl). Ann Sci For 46 S; Forest Tree Physiology (Dreyer E et al, eds) 443-447.
Jackson, R.B., Moore, L.A., Hoffmann, W.A., Pockman, W.T., Linder, C.R., 1999. Ecosystem rooting depth determined with caves and DNA. Proc. Natl. Acad. Sci. U.S. A. 96, 11387–11392.
Jackson, R.B., Sperry, J.S., Dawson, T.E., 2000. Root water uptake and transport: using physiological processes in global predictions. Trends Plant Sci. 5, 482–488.
Jiang, Z.C., Lian, Y.Q., Qin, X.Q., 2014. Rocky desertification in Southwest China: impacts, causes, and restoration. Earth-Sci. Rev. 132, 1–12.
Ksenzhek, O.S., Volkov, A.G., 1998. In: Plant Energetics. Elsevier Inc., pp. 243–266
Kumagai, T.O., Aoki, S., Shimizu, T., Otsuki, K., 2007. Sap flow estimates of stand transpiration at two slope positions in a Japanese cedar forest watershed. Tree Physiol. 27, 161–168.
Leonardi, S., Gentilesca, T., Guerrieri, R., Ripullone, F., Magnani, F., Mencuccini, M., Noije, T.V., Borghetti, M., 2012. Assessing the effects of nitrogen deposition and climate on carbon isotope discrimination and intrinsic water-use efficiency of angiosperm and conifer trees under rising CO_2 conditions. Glob Chang Biol. 18, 2925–2944.
Link, P., Simonin, K.A., Maness, H., Oshun, J., Dawson, T., Fung, I., 2014. Species differences in the seasonality of evergreen tree transpiration in a Mediterranean climate: analysis of multiyear, half-hourly sap flow observations. Water Resour. Res. 50, 1869–1894.
Liu, J., Shen, L., Wang, Z., Duan, S., Wu, W., Peng, X., et al., 2019. Response of plants water uptake patterns to tunnels excavation based on stable isotopes in a karst trough valley. J. Hydrol. 571, 485–493.
Liu, W., Wang, P., Li, J., Liu, W., Li, H., 2014. Plasticity of source water acquisition inepiphytic transitional and terrestrial growth phases of *Ficus tinctoria*. Ecohydrology 7, 1524–1533.
Liu, Z., Yu, X., Jia, G., 2018. Water utilization characteristics of typical vegetation in the rocky mountain area of Beijing, China. Ecol. Indic. 91, 249–258.
Martínez-Vilalta, J., Poyatos, R., Aguadé, D., Retana, J., Mencuccini, M., 2014. A new look at water transport regulation in plants. New Phytol. 204, 105–115.
McCole, A.A., Stern, L.A., 2007. Seasonal water use patterns of juniperus ashei on the Edwards Plateau, Texas, based on stable isotopes in water. J. Hydrol. 342 (3–4), 238–248.
McDonnell, J.J., 2014. The two water worlds hypothesis: ecohydrological separation of water between streams and trees? WIREs. Water 1, 323–329.
Millar, C., Pratt, D., Schneider, D.J., McDonnell, J.J., 2018. A comparison of extraction systems for plant water stable isotope analysis. Rapid Commun. Mass Spectrom. 32 (13), 1031–1044.
Miyazawa, Y., Tateishi, M., Komatsu, H., Ma, V., Kajisa, T., Sokh, H., Mizoue, N., Kumagai, T., 2014. Tropical tree water use under seasonal waterlogging and drought in central Cambodia. J. Hydrol. 515, 81–89.
Moore, J.W., Semmens, B.X., 2008. Incorporating uncertainty and prior information into stable isotope mixing models. Ecol. Lett. 11, 470–480.
Moreno-Gutiérrez, C., Dawson, T.E., Nicolás, E., Querejeta, J.I., 2012. Isotopes reveal contrasting water use strategies among coexisting plant species in a Mediterranean ecosystem. New Phytol. 196 (2), 489–496.
Muñoz-Villers, L.E., Friso, H., Susana, A.B.M., Geissert, D.R., Dawson, T.E., 2018. Reduced dry season transpiration is coupled with shallow soil water use in tropical montane forest trees. Oecologia 188, 1–15.
Nan, G.W., Wang, N., Jiao, L., Zhu, Y.M., Sun, H., 2019. A new exploration for accurately quantifying the effect of afforestation on soil moisture: a case study of artificial *Robinia pseudoacacia* in the Loess Plateau (China). Forest Ecol. Manage. 433, 459–466.
Nie, Y.P., Chen, H.S., Wang, K.L., Tan, W., Deng, P.Y., Yang, J., 2011. Seasonal water use patterns of woody species growing on the continuous dolostone outcrops and nearby thin soils in subtropical China. Plant Soil 341, 399–412.
Nie, Y.P., Chen, H.S., Wang, K.L., Yang, J., 2012. Water source utilization by woody plants growing on dolomite outcrops and nearby soils during dry seasons in karst region of Southwest China. J. Hydrol. 420–421, 264–274.
Nie, Y.P., Chen, H.S., Wang, K.L., Ding, Y.L., 2014. Seasonal variations in leaf $\delta^{13}C$ values: implications for different water-use strategies among species growing on continuous dolomite outcrops in subtropical China. Acta Physiol. Plant 36, 2571–2579.
Nobel, P.S., 2005. Physiochemical and Environmental Plant Physiology, 3rd edn. WH Freeman and Company, New York.
Nöjda, P., Korpela, M., Hari, P., Rannik, Ü., Sulkava, M., Hollmén, J., et al., 2017. Effects of precipitation and temperature on the growth variation of Scots pine—a case study at two extreme sites in Finland. Dendrochronologia 46, 35–45.
O'Leary, M.H., 1981. Carbon isotope fractionation in plants. Phytochemistry 20, 553–567.
Ogle, K., Tucker, C., Cable, J.M., 2014. Beyond simple linear mixing models: process-based isotope partitioning of ecological processes. Ecol. Appl. 24 (1), 181–195.
Olano, J.M., Linares, J.C., García-Cervigón, A.I., Arzac, A., Delgado, A., Rozas, V., 2014. Drought-induced increase in water-use efficiency reduces secondary tree growth and tracheid wall thickness in a Mediterranean conifer. Oecologia 176, 273–283.
Oren, R., Pataki, D.E., 2001. Transpiration in response to variation in microclimate and soil moisture in southeastern deciduous forests. Oecologia 127 (4), 549–559.
Orlowski, N., Frede, H.-G., Brüggemann, N., Breuer, L., 2013. Validation and application of a cryogenic vacuum extraction system for soil and plant water extraction for isotope analysis. J. Sens. 2, 179–193.
Osmond, C.B., Björkman, O., Anderson, D.J., 1980. Physiological processes in plant ecology. Springer, New York.
Parnell, A.C., Inger, R., Bearhop, S., Jackson, A.L., 2010. Source partitioning using stable isotopes: coping with too much variation. PLoS One 5, e9672.
Pataki, D.E., Oren, R., Smith, W.K., 2000. Sap flux of co-occurring species in a western subalpine forest during seasonal soil drought. Ecology 81 (9), 2557–2566.
Perrin, J., Jeannin, P.Y., Zwahlen, F., 2003. Epikarst storage in a karst aquifer: a conceptual model based on isotopic data, Milandre test site, Switzerland. J. Hydrol. 279 (1–4), 106–124.
Phillips, D.L., Gregg, J.W., 2001. Uncertainty in source partitioning using stable isotopes. Oecologia 127, 171–179.
Phillips, D.L., Gregg, J.W., 2003. Source partitioning using stable isotopes: coping with too many sources. Oecologia 136, 261–269.
Pockman, W.T., McElrone, A.J., Bleby, T.M., Jackson, R.B., 2008. The structure and function of roots of woody species on the Edwards Plateau, Texas, USA. Abstract H34A-02, Joint Assembly of American Geophysical Union, Ft. Lauderdale, FL.

Querejeta, J., Estrada-Medina, H., Allen, M., Jiménez-Osornio, J.J., Ruenes, R., 2006. Utilization of bedrock water by *Brosimum alicastrum* trees growing on shallow soil atop limestone in a dry tropical climate. Plant Soil 287, 187–197.

Querejeta, J., Estrada-Medina, H., Allen, M.F., Jimenze-Osornio, J.J., 2007. Water source partitioning among trees growing on shallow Karst soils in a seasonally dry tropical climate. Oecologia 152, 26–36.

Rong, L., Chen, X., Chen, X.H., Wang, S.J., Du, X.L., 2011. Isotopic analysis of water sources of mountainous plant uptake in a karst plateau of southwest China. Hydrol. Process. 25 (23), 3666–3675.

Rumman, R., Atkin, O.K., Bloomfield, K.J., Eamus, D., 2017. Variation in bulk-leaf 13C discrimination, leaf traits and water-use efficiency-trait relationships along a continental-scale climate gradient in Australia. Global Change Biology 24, 1186-1120.

Ryel, R.J., Ivans, C.Y., Peek, M.S., Leffler, A.J., 2008. Functional differences in soil water pools: a new perspective on plant water use in water-limited ecosystems. Prog. Botany 69, 397–422.

Ryel, R.J., Leffler, A.J., Ivans, C.Y., Peek, M.S., Caldwell, M.M., 2010. Functional differences in water-use patterns of contrasting life forms in great basin steppelands. Vadose Zone J. 9, 548–560.

Schultz, N.M., Griffis, T.J., Lee, X., Baker, J.M., 2011. Identification and correction of spectral contamination in $^{2}H/^{1}H$ and $^{18}O/^{16}O$ measured in leaf, stem, and soil water. Rapid Commun. Mass Spectrom. 25 (21), 3360–3368.

Schulze, E.-D., Kelliher, F.M., Korner, C., Lloyd, J., Leuning, R., 1994. Relationships among maximum stomatal conductance, ecosystem surface conductance, carbon assimilation rate, and plant nitrogen nutrition: a global ecology scaling exercise. Annu. Rev. Ecol. Syst. 25 (1), 629–660.

Schwarcz, H.P., 1991. Some theoretical aspects of isotope paleodiet studies. J. Archaeol. Sci. 18, 261–275.

Schwinning, S., 2008. The water relations of two evergreen tree species in a Karst savanna. Oecologia 158 (3), 373–383.

Schwinning, S., 2010. The ecohydrology of roots in rocks. Ecohydrology 3, 238–245.

Scott, R.L., Huxman, T.E., Williams, D.G., Goodrich, D.C., 2006. Ecohydrological impacts of woody-plant encroachment: ceasonal patterns of water and carbon dioxide exchange within a semiarid riparian environment. Global Change Biol. 12 (2), 311–324.

Seibt, U., Rajabi, A., Griffiths, H., Berry, J.A., 2008. Carbon isotopes and water use efficiency: sense and sensitivity. Oecologia 155, 441–454.

Semmens, B.X., Ward, E.J., Moore, J.W., Darimont, C.T., 2009. Quantifying inter- and intra-population niche variability using hierarchical Bayesian stable isotope mixing models. PLoS One 4 (7), e6187.

Sperry, J.S., Hacke, U.G., Oren, R., Comstock, J.P., 2002. Water deficits and hydraulic limits to leaf water supply. Plant. Cell Environ. 25, 251–263.

Stock, B.C., Semmens, B.X., 2013. MixSIAR GUI UserManual, Version 3.1. http://conserver. iugocafe.org/user/brice.semmens/MixSIAR.

Szutu, D.J., Papuga, S.A., 2019. Year-round transpiration dynamics linked with deep soil moisture in a warm desert shrubland. Water Resour. Res. 55, 5679–5695.

Wang, Q., Lintunen, A., Zhao, P., Shen, W., Salmon, Y., Chen, X., et al., 2020. Assessing environmental control of sap flux of three tree species plantations in degraded hilly lands in south china. Forests 11 (2), 206.

West, A.G., Goldsmith, G.R., Brooks, P.D., Dawson, T.E., 2010. Discrepancies between isotope ratio infrared spectroscopy and isotope ratio mass spectrometry for the stable isotope analysis of plant and soil waters. Rapid Commun. Mass Spectrom. 24 (14), 1948–1954.

White, J.W.C., Cook, E.R., Lawrence, J.R., Broecker, W.S., 1985. The D/H ratios of sap in trees: implications for water sources and tree ring D/H ratios. Geochim. Cosmochim. Acta 49, 237–246.

Wilson, K.B., Hanson, P.J., Mulholland, P.J., Baldocchi, D., Wullschleger, S.D., 2001. A comparison of methods for determining forest evapotranspiration and its components: sap-flow, soil water budget, eddy covariance and catchment water balance. Agric. For. Meteorol. 106, 153–168.

Xu, H., Li, Y., 2006. Water-use strategy of three central Asian desert shrubs and their responses to rain pulse events. Plant Soil 285, 5–17.

Yan, Y.J., Dai, Q.H., Wang, X.D., Li, J., Mei, L.N., 2019. Response of shallow karst fissure soil quality to secondary succession in a degraded karst area of southwestern China. Geoderma 348, 76–85.

Yan, C., Wang, B., Zhang, Y., Zhang, X., Takeuchi, S., Qiu, G., 2018. Responses of sap flow of deciduous and conifer trees to soil drying in a subalpine forest. Forests 9 (1), 32.

Yang, S.J., Zhang, Y.J., Goldstein, G., Sun, M., Ma, R.Y., Cao, K.F., 2015. Determinants of water circulation in a woody bamboo species: afternoon use and night-time recharge of culm water storage. Tree Physiol. 35, 964–974.

Yepez, E.A., Williams, D.G., Scott, R.L., Lin, G., 2003. Partitioning overstory and understory evapotranspiration in a semiarid savanna woodland from the isotopic composition of water vapor. Agric. For. Meteorol. 119 (1–2), 53–68.

Yuan, D.X., 1994. Karstology of China. Geological Publishing House, Beijing, China (in Chinese with English abstract).

Zheng, C., Wang, Q., 2014. Water-use response to climate factors at whole tree and branch scale for a dominant desert species in central Asia: Haloxylon ammodendron. Ecohydrology 7, 56–63.